Dynamic Self-Assembled Materials

Dynamic Materials through Metal-Directed and Solvent-Driven Self-Assembly of Cavitands**

*Laura Pirondini, Anna G. Stendardo, Silvano Geremia, Mara Campagnolo, Paolo Samorì, Jürgen P. Rabe, Roel Fokkens, and Enrico Dalcanale**

Reversibility constitutes one of the hallmarks of self-assembly.[1] This feature of self-assembled structures conveys many interesting properties, among which responsiveness to external stimuli is pivotal to the development of dynamic materials.[2] For this reason noncovalent interactions are being used increasingly in polymer science.[3] So far hydrogen bonding has been the workhorse of interactions, because it combines directionality with simplicity.[4] Metal–ligand coordination is another highly directional interaction that can lead to supramolecular polymeric architectures such as linear polymers[5] and dendrimers.[6] Hydrophobic interactions have also been exploited to form nanotube aggregates in aqueous solution.[7] However, to generate highly adaptive dynamic materials, systems operating in multimodal fashion through the implementation of several self-assembly codes are required.[8]

As a first step in this direction we report on the design, preparation, and properties of cavitand **1**, which is capable of bimodal, independent self-assembling interactions, namely solvophobic aggregation and metal coordination. The self-assembly cycle in Scheme 1 was devised to test the workability and orthogonality of the two interactions. For the first interaction the dimerization properties of quinoxaline kite velcrands have been exploited: the driving forces for dimerization are dipole–dipole, van der Waals, and solvophobic interactions.[9] For metal complexation two pyridine ligands have been introduced at the lower rim of **1** to induce dimerization through coordination to a metal center.[10] The two interactions operate under totally different sets of conditions allowing the independent activation/deactivation of each of them.

The kite monomer **1** was synthesized by condensing 2,3-dichloroquinoxaline with a tetramethylhydroxyl-footed resorcinarene[10,11] to afford the corresponding quinoxaline-bridged cavitand, which was then treated with 3,5-bis(chlorocarbonyl)pyridine in pyridine (see Supporting Information for experimental details and characterization of new compounds). The reaction led to the formation of **1** in 28% yield. Cavitand **1** is soluble only in chlorinated and aromatic hydrocarbons at relatively high dilution ($c < 2.2$ mM). Of the two possible isomers, only that in which the pyridyl moieties are under the *out*-phenyls of the resorcinarene skeleton is formed.[12]

Kite-to-kite dimerization in CD_2Cl_2 solution was monitored by ^{1}H NMR spectroscopy by following the splitting of several diagnostic signals (see Supporting Information). The association–dissociation rates for the monomer and dimer are fast on the ^{1}H NMR timescale at room temperature but slow below 240 K. At that temperature two different sets of signals appear, belonging to the monomer and dimer in slow exchange. The populations of the two species can be determined directly by integration of their respective signals, which provides a convenient means of determining association constants (K_a) and free energies of association over a range of temperatures (235–205 K).[13] The following thermodynamic parameters were determined: $K_{a273K} = 1.91 \times 10^3\,\text{M}^{-1}$; $\Delta G^{\circ}_{273K} = -4.10$ kcal mol^{-1}; $\Delta H = -0.66$ kcal mol^{-1}, $\Delta S = 12.6$ cal mol^{-1} K^{-1} (correlation factor in van't Hoff plot: 0.9523).

These data, compared with those of the related tetrapentyl-footed kite velcrand **HQx**,[9] indicate a reduced tendency of **1** to dimerize ($\Delta G^{\circ}_{\mathbf{HQx}} = -6.81$ kcal mol^{-1} versus $\Delta G^{\circ}_{\mathbf{1}} = -4.10$ kcal mol^{-1} calculated at 273 K). As shown by the X-ray crystal structure[14] (Figure 1) a **1**·**1** velcrand dimer forms in the solid state, in which the two cavitands are rotated reciprocally by 90°: two methyl groups are oriented outward and the other two point upward, fitting into the cavities formed by the sloping aryl faces and the "out" methyl groups. When two molecules are fitted to one another they share a large common surface formed by their large rectangular areas in roughly parallel planes. The introduction of two pyridyl-based connecting units at the lower rim rigidifies the structure, affecting the spatial orientation of the quinoxaline wings and therefore reducing the tendency to dimerize. This is confirmed by the crystal structure of **1**·**1**, which evidences only 77 short intermolecular atomic distances, remarkably less than the 132 short distances observed in **HQx**·**HQx** (see Supporting Information).[15] Besides, the crystal packing reveals that in the solid state the pyridyl terminal groups act as clips, forming linear chains of **1**·**1** dimers through stacking interactions (Scheme 1).

Metal-directed dimerization has been already performed on the corresponding methylene-bridged cavitand, by using

[*] Prof. E. Dalcanale, Dr. L. Pirondini, Dr. A. G. Stendardo
Dipartimento di Chimica Organica ed Industriale and Unità INSTM
Università degli Studi di Parma
Parco Area delle Scienze 17/A, 43100 Parma (Italy)
Fax: (+39) 0521-905-472
E-mail: enrico.dalcanale@unipr.it

Prof. S. Geremia, Dr. M. Campagnolo
Centro di Eccellenza in Biocristallografia
Dipartimento di Scienze Chimiche, Università di Trieste
Via L. Giorgieri 1, 34127 Trieste (Italy)

Dr. P. Samorì, Prof. J. P. Rabe
Humboldt University Berlin, Department of Physics
10099 Berlin (Germany)

Dr. R. Fokkens
Laboratory of Supramolecular Chemistry and Technology
MESA+ Research Institute, University of Twente
P.O. Box 217, 7500 AE Enschede (The Netherlands)

[+] Present address:
Istituto per la Sintesi Organica e la Fotoreattività
C.N.R. Bologna, Via Gobetti 101
40129 Bologna (Italy)

[**] We acknowledge the CNR Nanotechnology Programme for financial support. We thank Dr. Nikolai Severin for help in preparing the thin films.

Supporting information for this article is available on the WWW under http://www.angewandte.org or from the author.

 © 2003 Wiley-VCH Verlag GmbH & Co. KGaA, Weinheim 0044-8249/03/11512-1422 $ 20.00+.50/0

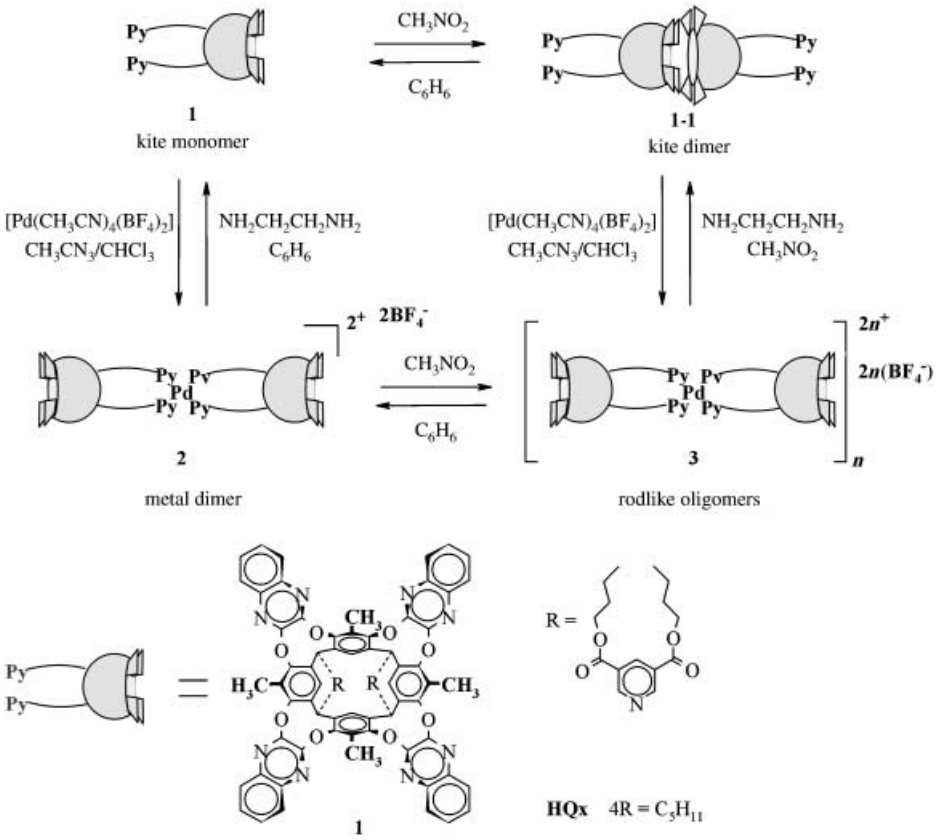

Scheme 1. Bimodal self-assembly cycle.

$[Pd(CH_3CN)_4](BF_4)_2$ as the metal precursor (see Supporting Information).[10] Addition of a small excess of a bidentate competitive ligand such as ethylenediamine to the preformed complex led to complete and clean disassembly of the coordination dimer, which proves the reversibility of the metal-directed dimerization process.

The two self-assembly protocols were combined to generate new oligomeric structures by mixing **1** and $[Pd(CH_3CN)_4](BF_4)_2$ in a 2:1 molar ratio in $CHCl_3/CH_3CN$.

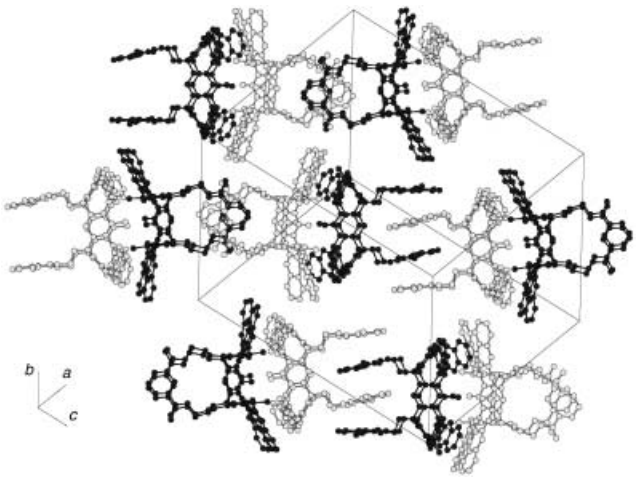

Figure 1. X-ray crystal structure of the **1**·**1** dimer.

Complex **3** precipitated as a yellow powder, soluble only in nitromethane. The ^1H NMR spectrum of **3** in CD_3NO_2 shows both a broadening and an increased number of peaks, indicative of the formation of oligomeric species. A downfield shift of the peaks relative to the pyridine protons from $\delta = 9.20$ ppm (**1** in CD_2Cl_2) to $\delta = 9.80$ ppm (**3** in CD_3NO_2) was observed, which is diagnostic of coordination to the metal center. The MALDI-TOF mass spectrum of **3**[16] in CH_3NO_2 shows three singly charged ion peaks at *m*/*z* 3279.2, 6648.6, and 10016.3 attributable to $[\mathbf{1}\cdot Pd(BF_4)_2\cdot\mathbf{1}\text{-}BF_4^-]^+$, $[(\mathbf{1}\cdot Pd(BF_4)_2\cdot\mathbf{1})_2\text{-}BF_4^-]^+$, and $[(\mathbf{1}\cdot Pd(BF_4)_2\cdot\mathbf{1})_3\text{-}BF_4^-]^+$, which belong to the species with $n = 1$, $n = 2$, and $n = 3$, respectively (see Supporting Information). The laser ionization process was kept at threshold level to avoid molecular clustering in the gas phase.

Clean solvophobic disassembly was observed by dissolving complex **3** in [D_6]benzene.[17] The resulting ^1H NMR spectrum shows sharp and easily assignable peaks belonging to the dimeric species **2**. This attribution was confirmed by a MALDI-TOF MS experiment performed on a solution of complex **3** in benzene,[16] in which only the single charged ion peak at *m*/*z* 3279.2 ($[\mathbf{1}\cdot Pd(BF_4)_2\cdot\mathbf{1}\text{-}BF_4^-]^+$) attributable to dimer **2**, is revealed.

Coordinative disassembly of **3** has been carried out through addition of ethylenediamine to break selectively the oligomeric species at the metal coordination sites. Depending on the solvent used, either **1** (in benzene) or **1**·**1** (as a precipitate from nitromethane) were recovered, proving

the complete reversibility of the metal-directed self-assembly at the lower rim.

The self-assembly of these supramolecular architectures on surfaces has also been explored, by making use of tapping mode scanning force microscopy (TM-SFM). When **3** was deposited from dilute solution in CH_3NO_2 onto the basal plane of highly oriented pyrolytic graphite (HOPG), large disordered assemblies were obtained (image not shown). To avoid lateral aggregation between individual self-assembled objects, a linear alkane ($C_{32}H_{64}$) was added to the dilute solution (ca. 10^{-3} M) of **3** in CH_3NO_2 up to saturation. Upon application of this solution to a graphite surface the two solutes are codeposited.[5d] Due to the strong affinity between the alkanes and the HOPG surface,[18] the alkanes pack in lamellar 2D single crystals, with the long molecular axes parallel to the substrate and extended over several hundreds of nanometers. After the liquid was removed by spinning off in a spin-coater, the films were thermally annealed at 40 °C for 15 min, which led to complete solvent evaporation. The SFM image in Figure 2a shows different types of nanostructures

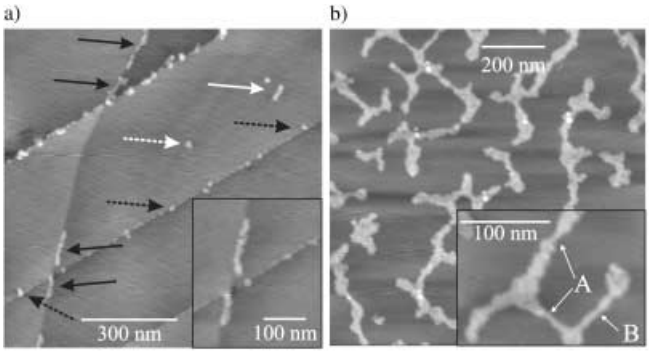

Figure 2. Trapping mode STM images of self-assembled **3** codeposited with linear alkanes from a CH_3NO_2 solution.

coexisting on the graphite surface. Rodlike (solid arrows) and grainlike objects (dashed arrows) can be recognized. Both of them are preferentially packed at the graphite steps (black arrows), although they can also exist on a flat graphite terrace (white arrows). The inset in Figure 2a gives a closer look at two rodlike objects at a graphite step. A single self-assembled object is expected to exhibit a rodlike shape with a cross-section diameter ranging from 0.8 (coordination site) to 1.5 nm (solvophobic site).

The observed anisotropic objects exhibit heights of roughly (0.8 ± 0.2) nm, lengths of up to 150 nm, and widths of (7 ± 3) nm,[19] which is consistent with the lateral aggregation of five to seven supramolecular rods.[20] Different areas of the same film are characterized by a higher degree of coverage, leading to networks with heights of (0.8 ± 0.2) nm or multiples thereof. The inset in Figure 2b exhibits some narrow arms with constant widths of 1.5 nm, which is compatible with a single rod having a height of about 0.8 nm (monolayer, marked with A) or 1.5 nm (bilayer, indicated with B).[21,22]

In summary we have devised and tested a bimodal self-assembly protocol for the generation of a dual-coded dynamic supramolecular species, which has been transferred and amplified on surfaces. The two interaction modes are both orthogonal and reversible, as proven by the self-assembly cycle of Scheme 1, where the formation/dissolution of either dimers or oligomers has been triggered by solvent polarity, metal coordination, and ligand exchange. This result can be of importance in the frame of the implementation of new materials with the peculiar properties of adaptability, healing, and response to external stimuli.

Received: October 14, 2002 [Z50352]

Keywords: cavitands · dynamic materials · nanostructures · self-assembly · supramolecular chemistry

[1] J. S. Lindsey, *New J. Chem.* **1995**, *15*, 153 – 180.
[2] a) J.-M. Lehn in *Supramolecular Science: Where It Is and Where It Is Going* (Eds.: R. Ungaro, E. Dalcanale), Kluwer Academic Publishers, Dordrecht, **1999**, 287 – 304; b) J.-M. Lehn, *Chem. Eur. J.* **1999**, *5*, 2455 – 2463.
[3] a) N. Zimmerman, J. S. Moore, S. C. Zimmerman, *Chem. Ind.* **1998**, 604 – 610; b) *Supramolecular Polymers* (Ed.: A. Ciferri), Dekker, New York, **2000**.
[4] a) R. P. Sijbesma, F. H. Beijer, L. Brunsveld, B. J. B. Folmer, J. H. K. K. Hirschberg, R. F. M. Lange, J. K. L. Lowe, E. W. Meijer, *Science* **1997**, *278*, 1601 – 1604; b) R. K. Castellano, D. M. Rudkevich, J. Rebek, Jr., *Proc. Natl. Acad. Sci. USA* **1997**, *94*, 7132 – 7137; c) R. K. Castellano, J. Rebek, Jr., *J. Am. Chem. Soc.* **1998**, *120*, 3657 – 3663.
[5] a) U. Michelsen, C. A. Hunter, *Angew. Chem.* **2000**, *112*, 780 – 783; *Angew. Chem. Int. Ed.* **2000**, *39*, 764 – 767; b) L. Brunsveld, B. J. B. Folmer, E. W. Meijer, R. P. Sijbesma, *Chem. Rev.* **2001**, *101*, 4071 – 4097; c) U. S. Schubert, C. Eschbaumer, *Angew. Chem.* **2002**, *114*, 3016 – 3050; *Angew. Chem. Int. Ed.* **2002**, *41*, 2892 – 2926; d) D. G. Kurth, N. Severin, J. P. Rabe, *Angew. Chem.* **2002**, *114*, 3833 – 3835; *Angew. Chem. Int. Ed.* **2002**, *41*, 3681 – 3683.
[6] a) W. T. S. Huck, F. C. J. M. van Veggel, B. L. Kropman, D. H. A. Blank, E. G. Keim, M. M. A. Smithers, D. N. Reinhoudt, *J. Am. Chem. Soc.* **1995**, *117*, 8293 – 8294; b) W. T. S. Huck, F. C. J. M. van Veggel, D. N. Reinhoudt, *Angew. Chem.* **1996**, *108*, 1304 – 1306; *Angew. Chem. Int. Ed. Engl.* **1996**, *35*, 1213 – 1215.
[7] G. Li, L. B. McGown, *Science* **1994**, *264*, 249 – 251.
[8] J.-M. Lehn, *Science* **2002**, *295*, 2400 – 2403.
[9] a) J. R. Moran, J. L. Ericson, E. Dalcanale, J. A. Bryant, C. B. Knobler, D. J. Cram, *J. Am. Chem. Soc.* **1991**, *113*, 5707 – 5714; b) D. J. Cram, H.-J. Choi, J. A. Bryant, C. B. Knobler, *J. Am. Chem. Soc.* **1992**, *114*, 7748 – 7765.
[10] L. Pirondini, D. Bonifazi, E. Menozzi, E. Wegelius, K. Rissanen, C. Massera, E. Dalcanale, *Eur. J. Org. Chem.* **2001**, 2311 – 2320.
[11] B. C. Gibb, R. G. Chapman, J. C. Sherman, *J. Org. Chem.* **1996**, *61*, 1505 – 1509.
[12] No kite-to-kite interconversion to give the other isomer has been observed by dynamic ^{1}H NMR spectroscopy up to 373 K.
[13] K_a can be calculated by $K_a = R(2R+1)/[M]_i$, where $R = 0.5$ (integral value of dimer)/(integral value of monomer), and $[M]_i$ is the initial concentration of monomer.
[14] Crystals of **1** suitable for X-ray analysis were grown in EtOH/CH_2Cl_2 solution. Crystal data: $2(C_{90}H_{66}N_{10}O_{16})\cdot 0.5(C_6H_{14}O_4)\cdot 1.5(C_4H_{10}O_3)\cdot 8.5\,C_2H_6O\cdot 6H_2O$, $M_r = 3821$, monoclinic, space group $P2_1/n$, $a = 25.525(5)$, $b = 25.003(5)$, $c = 33.306(5)$ Å, $\beta = 91.58(5)°$, $V = 21248(7)$ Å^3, $Z = 4$, $\rho_{calcd} = 1.194$ mg m^{-3}, $\mu = 0.72$ mm^{-1}, $F(000) = 8068$, $\lambda/2\theta_{max} = 0.95$ Å. A total of 81624 reflections were measured, of which 23203 were

 © 2003 Wiley-VCH Verlag GmbH & Co. KGaA, Weinheim 0044-8249/03/11512-1424 $ 20.00+.50/0

unique ($R_{int} = 0.053$). To solve the structure 19441 reflections were used (parameters = 2338, $R1[I > 2\sigma(I)] = 0.1541$, $wR2 = 0.4125$). Data collection was performed at the X-ray diffraction beamline of Elettra Synchrotron, Trieste (Italy) (monochromatic wavelength $\lambda = 1.0000$ Å), by using a Mar CCD detector with the rotating crystal method. The crystal was soaked with an aqueous solution of PEG 1000 (100% g mL^{-1}) (used as cryoprotectant), mounted in a loop, and flash-frozen to 100 K. The diffraction data were indexed and integrated using MOSFLM and scaled with SCALA. The structure was solved by direct methods (SIR97) and Fourier analyses, and refined by full-matrix least-squares based on F^2 (SHELXL-97). Several solvent molecules were detected in the asymmetric unit: 0.5 molecules of triethyleneglycol, 1.5 molecules of diethyleneglycol, 8.5 molecules of ethanol, and 6 water molecules. CCDC-194186 contains the supplementary crystallographic data for this paper. These data can be obtained free of charge via www.ccdc.cam.ac.uk/conts/retrieving.html (or from the Cambridge Crystallographic Data Centre, 12, Union Road, Cambridge CB2 1EZ, UK; fax: (+44) 1223-336-033; or deposit@ccdc.cam.ac.uk).

[15] The average contribution to the free energy of each contact is 0.053 kcal mol^{-1}, which is in full agreement with the reported value for Cram's **HQx**·**HQx** system (0.053 kcal mol^{-1}).

[16] The spot wells of the MALDI-TOF sample plate containing millimolar solutions of the assemblies in different solvents were covered with a thin poly(ethyleneglycol) film. In this way the original constitution of the sample solutions is mostly preserved, and evaporation is kept to a minimum.

[17] For the opposite behavior in hydrogen-bonded velcrands see: F. C. Tucci, D. M. Rudkevich, J. Rebek, Jr., *Chem. Eur. J.* **2000**, *6*, 1007 – 1016.

[18] J. P. Rabe, S. Buchholz, *Science* **1991**, *253*, 424 – 427.

[19] The rod widths were determined by taking into account the broadening due to the convolution with the SFM tip, as described in: P. Samorí, V. Francke, K. Müllen, J. P. Rabe, *Chem. Eur. J.* **1999**, *5*, 2312 – 2317.

[20] The individual supramolecular rods could not be resolved due to the limitation in the SFM resolution and to their tight packing.

[21] As in the case of polyelectrolyte–amphiphile complexes,[5d] the cavitand-based supramolecular polymer is very likely lying on the top of an alkane monolayer (SAM) self-assembled on HOPG, taking advantage of the high surface potential ripple of the underlying SAM.

[22] The apparent rod thickness of 0.8 nm is at the lower end of the expected range. This can be due to both the flattening at surfaces occurring upon adsorption and to imaging artifacts. The latter can include indentation of the supramolecular object by the probing tip as well as the adhesion of the tip to the surface as discussed in: P. Samorí, C. Ecker, I. Gössl, P. A. J. de Witte, J. J. L. M. Cornelissen, G. A. Metselaar, M. B. J. Otten, A. E. Rowan, R. J. M. Nolte, J. P. Rabe, *Macromolecules* **2002**, *35*, 5290 – 5294.